

FORWARD MODELING OF THE GEOID ANOMALY USING SPHERICAL
HARMONICS: APPLICATIONS IN THE SIERRA NEVADA

by

Alissa C Scire

A Prepublication Manuscript Submitted to the Faculty of the

DEPARTMENT OF GEOSCIENCES

In Partial Fulfillment of the Requirements
for the Degree of

MASTER OF SCIENCE

In the Graduate College
THE UNIVERSITY OF ARIZONA

2010

Forward modeling of the geoid anomaly using spherical harmonics: Applications in the Sierra Nevada

A. Scire¹ and C. G. Chase¹

¹Department of Geosciences, University of Arizona

Abstract

This paper discusses the initial tests of a forward modeling technique using topography to calculate the geoid anomaly. Since geoid anomalies can be used to determine a non-unique density structure of the Earth, they are one tool that can be used to explore crustal structure and thickness. Using spherical harmonics is appropriate because the same filter can be applied to both the modeled geoid anomaly and the observed geoid anomaly to allow comparison between the two. Since the primary focus of the model is on crustal contributions to the geoid anomaly, the harmonics related to deep mantle sources are filtered out, using a cosine-tapered high-pass filter, leaving only higher order harmonics corresponding to crustal contributions to the geoid anomaly. Since the degree and mechanism of isostatic compensation is of interest in studying any mountain range, the initial application of the model assumes Airy-style isostatic compensation of the topography of the Sierra Nevada Mountains to test the utility of the forward model. The comparison of the modeled geoid anomaly assuming a 30 km reference crustal thickness to the observed geoid anomaly indicate that purely Airy-style crustal compensation of the Sierra Nevada is unable to reproduce the amplitude of the observed geoid anomaly. Additional models run using thicker reference crusts to simulate compensation in the mantle also fail to reproduce the observed amplitude, indicating that other mechanisms of compensation for the Sierra Nevada beyond Airy-style isostatic compensation need to be explored.

Introduction

This paper discusses the implementation of a forward model used to calculate the geoid anomaly for a specified region. The model assumes that the topography of a given region is isostatically compensated in the crust, ignoring mantle contributions to isostatic compensation for the initial model. The forward model uses spherical harmonics to calculate the geoid anomaly. The modeled geoid anomaly can then be compared to the observed geoid anomaly to discuss the contribution of the crust to the isostatic compensation of a region. This forward model is applied to the Sierra Nevada Mountains as an initial test region to demonstrate the utility of the model. The Sierra Nevada is utilized as a test region because of the limited scale of the mountain belt and the wide range of work that has been done in the region, providing a substantial base of information.

Background: The geoid and geoid anomaly

The geoid is defined as an equipotential surface of the Earth's gravity field. The reference geoid is the equipotential surface that corresponds to mean sea level. Deviations from the reference geoid are called geoid anomalies and correspond to mass excesses or deficits in the subsurface due to density variations relative to the reference density. Geoid anomalies are related to the gravitational potential by dividing the anomalous gravitational potential by the reference gravity, or

$$N(\varphi, \theta) = \frac{T(\varphi, \theta)}{\gamma(\varphi)} \quad (1)$$

where N is the geoid anomaly, $T(\varphi, \theta)$ is the anomalous gravitational potential as a function of colatitude φ and longitude θ , and $\gamma(\varphi)$ is the reference gravity as a function of colatitude (Heiskanen and Moritz, 1967).

The geoid anomaly can be a useful tool to study density distributions in the Earth. However, the solution to a geoid anomaly inversion is non-unique, with an infinite number of mass configurations producing the same geoid anomaly (Featherstone, 1997). While this does not invalidate geoid anomaly studies as a geophysical research tool, it needs to be considered when evaluating the results of any geoid anomaly study.

Background: Isostasy

One of the primary assumptions of the model as discussed in this paper is the assumption of Airy isostatic compensation. In an Airy isostatic model, topography is compensated by the presence of a crustal root, thickening the crust beneath a region of higher topography (Figure 1). The thickness of the crust can be calculated for a region by assuming Airy isostatic compensation. While this is not a valid assumption everywhere, Airy isostasy acts as an end member case for the initial implementation of the model. The thickness of the crustal root, h_b , in an Airy isostatic model is

$$h_b = \frac{\rho_c \varepsilon_c}{(\rho_m - \rho_c)} \quad (2)$$

where ε_c is the elevation above sea level at a given point. The model assumes a uniform crust, with density $\rho_c = 2750 \text{ kg/m}^3$ and a reference crustal thickness $h_r = 30 \text{ km}$ (Table 1). Similarly, the thickness of the crustal root h_b for topography with a negative height h_w (i.e. below sea level; see Figure 1) is

$$h_b = h_w \left(\frac{\rho_c - \rho_w}{\rho_m - \rho_c} \right) \quad (3)$$

where ρ_w is the density of water and the other variables are defined in Table 1.

The model and its components

The model discussed in this paper calculates the geoid anomaly for a given region assuming that isostatic compensation occurs in the crust. This forward model calculates spherical harmonic coefficients for a point (the field point) on the Earth's surface and then uses the coefficients to determine the geoid anomaly at the field point. The geoid anomaly at each field point includes the contributions to the geoid anomaly from topography within a specified radius of the field point as well as the contribution of the topography at the field point (Figure 2). The following section discusses the model in detail, including assumptions made in the model and the limitations of both the model and the output.

The model and its components: Spherical harmonic calculation of the geoid anomaly

The forward model uses a spherical harmonic representation to calculate the geoid anomaly. While the geoid anomaly can be calculated without the use of a spherical harmonic framework, the spheroidal nature of the Earth lends itself readily to calculations in a spherical coordinate system. Using spherical harmonics also allows the same filter to be applied to the observed geoid anomaly and the modeled geoid anomaly. The major disadvantage of a spherical harmonic framework is the computational requirements of the calculation. The number of coefficients calculated for a given maximum degree of an analysis goes as $(n_{\max} + 1)^2$ (Chase, 1985). The computational requirements are important because the degree n of the analysis determines the limits on the resolution of the solution. The resolution of a spherical harmonic analysis is discussed in more detail later.

The geoid anomaly at each point is represented by the equation

$$N(r, \varphi, \theta) = \frac{GM_e}{r\gamma(\varphi)} \sum_{n=1}^{\infty} \left(\frac{r_e}{r}\right)^n \sum_{m=0}^n [\bar{J}_{nm} \cos m\theta + \bar{K}_{nm} \sin m\theta] \bar{P}_{nm}(\mu) \quad (4)$$

where the symbols are defined in Table 2. Equation (4) represents the geoid anomaly at the field point due to the ensemble of mass anomalies surrounding the field point. The potential coefficients J_{nm} and K_{nm} represent sum of the effects of the mass anomalies surrounding the field point. Sutton et. al (1991) defines these coefficients as the sum of the coefficients of each of the k mass points comprising the ensemble of mass anomalies, or

$$\begin{bmatrix} \bar{J}_{nm} \\ \bar{K}_{nm} \end{bmatrix} = \sum_{i=1}^k \begin{bmatrix} i\bar{J}_{nm} \\ i\bar{K}_{nm} \end{bmatrix} \quad (5)$$

where the coefficients of the individual mass elements are denoted by the index i . For the case of the forward model discussed here, the radius of influence around the field point of mass anomalies is defined as 1 arc-degree. After testing the model, it was determined that mass anomalies farther than 1 arc-degree away from the field point for a topographic grid having a

resolution of 10 arc-minutes have a negligible effect on the geoid anomaly at the field point. For coarser grids this distance would have to be modified since each point in a coarser grid would correspond to a larger mass, resulting in each point having a stronger influence on the surrounding points. This does cause problems near the poles as the distance of 1 degree of longitude decreases and would need to be adjusted to model regions near the North or South poles.

The model and its components: Degree and order

The spherical harmonic framework uses two indices, resulting from the dependence of the solution on both colatitude and longitude. For the purpose of this paper, n is defined as the degree while m is defined as the order. For gravity studies, the degree of the analysis is particularly important. Higher degree harmonics correspond to increasingly more detailed representations of the geoid anomaly. The non-unique nature of the geoid anomaly inversion prevents any definitive determinations being made about the relationship between the harmonic degree and the depth of the causative mass anomalies. However, some general statements about the relationship between harmonic degree and the depth of mass anomalies can be made. Several papers have explored the correlation between the spherical harmonic degree and the depth of the causative mass anomalies. The degree 2 and 3 harmonics correspond primarily to sources at or near the core-mantle boundary (Bowin 1983). A study by Hager (1984) indicates that the degree 4 to 9 harmonics are correlated with density models of subducted slab. Although the radial distribution of anomalous masses cannot be uniquely determined, large, deep sources appear to produce the lower degree harmonics while higher degree harmonics are probably produced by smaller, shallower sources (Jackson et. al., 1991).

Although the solution to the geoid anomaly inversion is non-unique, an estimate of the maximum depth of sensitivity for a give harmonic degree can be made. The maximum depth of sensitivity of each spherical harmonic degree is

$$z_{max} = \frac{r_e}{n - 1} \quad (6)$$

as defined by Bowin et. al. (1986). Featherstone (1997) points out that this relationship between depth and spherical harmonic degree does not preclude any contribution to the geoid anomaly from shallower sources due to the non-uniqueness of the geopotential field inversion. Therefore, Equation (6) only offers an upper limit on the depth of a mass anomaly. However, due to the nature of the relationship between the maximum depth of a mass anomaly and the degree of the analysis, limiting the depth sensitivity of a spherical harmonic solution becomes a tradeoff between the depth sensitivity and the computational demand of the analysis. Limiting the depth sensitivity to shallow depths requires a large minimum degree of the analysis (Figure 3a).

Similarly, the wavelength of the detectable geoid anomaly features at the surface of the Earth is also dependent on the spherical harmonic degree. The wavelength λ of the geoid anomaly features at the Earth's surface is

$$\lambda = \frac{2\pi r_e}{n} \quad (7)$$

where λ is in kilometers (Bowin et. al., 1986). Lower degree harmonics correspond to longer wavelength features of the geoid anomaly while increasing the harmonic degree decreases the wavelength, allowing for more detailed representations of the geoid anomaly. Like the depth sensitivity of the solution, increasing the wavelength sensitivity of a spherical harmonic analysis requires higher maximum degrees of the analysis, resulting in greater computational demands of the model (Figure 3b). Since increasing the maximum degree of the spherical harmonic solution results in a significant increase in the number of coefficients calculated (Figure 3c), increasing the resolution of the solution quickly increases the computational demands of the analysis.

Since the forward model discussed here models geoid anomalies due to crustal mass anomalies, the lower degree harmonics are discarded from the geoid anomaly solution to remove the contribution to the geoid anomaly of mass anomalies in the lower mantle and the core. This also allows for shorter wavelength features to be modeled and reduces the influence of long-wavelength geoid anomaly features.

The model and its components: The coefficients and topography as a point dipole

The coefficients for the spherical harmonic framework depend on the geometry of the model of the mass anomalies. Pollack (1973) lays out the equations for the coefficients for mass anomalies modeled as a point mass, a spherical cap and a spherical rectangle at the surface of a sphere, and Sutton et. al. (1991) extends these models to calculate the coefficients for volumetric elements with the same surficial shape. For the case of the forward model discussed here, we are only concerned with two of these models. Pollack (1973) initially determined the equation for the coefficients of a point mass at the surface of a sphere. Sutton et. al. (1991) generalized this equation for a point mass located at any radius within the sphere. The coefficients of a point mass at any radius r_i within a sphere are given by

$$\begin{bmatrix} \bar{J}_{nm} \\ \bar{K}_{nm} \end{bmatrix} = \frac{-1}{2n+1} \left(\frac{r_i}{r_e}\right)^n \left(\frac{M_i}{M_e}\right) \begin{bmatrix} \bar{R}_{nm}(\mu_i, \theta_i) \\ \bar{S}_{nm}(\mu_i, \theta_i) \end{bmatrix} \quad (8)$$

where \bar{R}_{nm} and \bar{S}_{nm} are fully normalized surface spherical harmonic functions defined as

$$\begin{bmatrix} \bar{R}_{nm}(\mu_i, \theta_i) \\ \bar{S}_{nm}(\mu_i, \theta_i) \end{bmatrix} = \bar{P}_{nm}(\mu_i) \begin{bmatrix} \cos(m\theta_i) \\ \sin(m\theta_i) \end{bmatrix} \quad (9)$$

(Sutton et. al., 1991). While the representation of mass anomalies due to topography as point masses might be appropriate in some cases, Sutton et. al (1991) argues that isostatically

compensated topography, with a thick crustal root below high topography, might be better represented by a different model. For this forward model, topography that is compensated by an Airy isostatic root is represented as a point dipole, with the elevation above sea level acting as a positive anomalous mass M_i^+ and the crustal root acting as the negative balancing mass M_i^- . The coefficients for a point dipole at an arbitrary radius r_i within the Earth are given by

$$\begin{bmatrix} \bar{J}_{nm} \\ \bar{K}_{nm} \end{bmatrix} = \left(\frac{-n}{2n+1} \right) \left(\frac{r_i}{r_e} \right)^n \left(\frac{M_i}{M_e} \right) \left(\frac{d}{r_i} \right) \begin{bmatrix} \bar{R}_{nm}(\mu_i, \theta_i) \\ \bar{S}_{nm}(\mu_i, \theta_i) \end{bmatrix} \quad (10)$$

where d is the distance between the anomalous mass and the compensating mass (Sutton et. al., 1991). For the case of Airy isostasy, the disturbing mass is compensated by the thick crustal root, making the distance between the masses d equal to the crustal thickness h_c . While the scaling term $-n/(2n+1)$ for the point dipole asymptotically approaches $1/2$, making the scaling term for the point dipole (Equation 10) larger in the higher-degree harmonics than the point mass (Equation 8), the distance between the disturbing mass and the compensating mass d is much smaller than the distance from the coordinate origin to the disturbing mass r_i . This results in the point dipole having less strength than the point mass, particularly in the lower harmonic degrees (Sutton et. al., 1991).

Data: The Sierra Nevada, topography, and crustal thickness

The region chosen for the initial test of the model is the Sierra Nevada on the border between California and Nevada (Figure 4). The specific area chosen lies between 35 and 41°N and 117 and 122°W. This area represents some of the highest topography of the Sierra Nevada including Mount Whitney, the highest point in the contiguous United States. Seismic studies in the area have led to insight into the structure of the crust and the depth of the Moho and have led to questions about the mechanism of support for the Sierra Nevada. The highest topography of the Sierra Nevada does not appear to be underlain by the thickest crust. According to Ruppert et. al. (1998), the crust beneath the crest of the Sierra Nevada Mountains is about 35 km thick. This is about 10 km thinner than the crustal thickness predicted by the Airy isostatic model used here (Figure 5). Seismic studies indicate that the thickest crust underneath the Sierra Nevada mountains lies to the west of the crest of the Sierras under the western slopes of the range (Fliedner et. al., 1996; Ruppert et. al., 1998; Fliedner et. al., 2000). While this indicates that the Sierra Nevada Mountains are not underlain by an Airy-style crustal root, the assumption of Airy isostatic compensation can be tested as an end member case.

The topography data used as the input for the forward model is from the ETOPO2v2 data set which is a 2 arc-minute global topographic grid. Due to the computational demands of the model, the resolution of the input data was reduced to a 10 arc-minute grid or approximately 20 kilometers. Finer resolution was not felt to be necessary for the purpose of this model. The topographic data set for the region of study, with boundaries stated above, was used to calculate a predicted crustal thickness below sea level assuming isostatic compensation by Airy isostasy

(Equations 2 and 3). Figure 5 shows the predicted crustal thickness assuming that the reference crust is 30 kilometers thick used in the forward model. The forward model then uses the input data set and the predicted crustal thickness to calculate the geoid anomaly as discussed in the previous section.

Results: The calculated and observed geoid anomalies

The calculated and observed geoid anomalies can be seen in Figure 6. Both the observed and the modeled geoid anomaly are displayed using the same color scale. The observed geoid anomaly (Figure 6a) is calculated from the EGM2008 spherical harmonic coefficient data set (Pavlis et. al, 2008). The calculated geoid anomaly was calculated using the program written using Matlab discussed in detail previously with the assumption of crustal Airy isostatic compensation and using the spherical harmonic coefficients calculated using a point dipole model (Equation 10). In order to make a legitimate comparison between the observed and modeled geoid anomalies, both are calculated using the same range of harmonic degrees. Also, both data sets have been filtered using the same cosine-tapered filter applied to the first and last five harmonic degrees of both the modeled and observed geoid. The minimum degree of the analysis was set to $n = 70$ with the upper end of the filter set at $n = 75$. From Equation (6), the maximum depth of causative mass anomalies that the harmonic analysis is sensitive to is about 92 kilometers. As an initial filter, this is a reasonable maximum depth of causative mass anomalies since the forward model is focused on crustal contributions to the geoid anomaly. Higher degree filters would correspond to progressively shallower depths, allowing for a better determination of the crustal contributions to the geoid anomaly to be determined. Similarly, the maximum degree was set to $n = 905$ with the lower end of the filter set to $n = 900$. While this does not give information about the minimum depth of causative mass anomalies because of the non-unique nature of geoid anomaly inversions, it does give constraints on the minimum wavelength sensitivity as defined in Equation (7). The analysis is sensitive to geoid anomalies with wavelengths of about 0.4 arc-degrees or about 44 kilometers. Higher degree analyses could provide information about lower wavelength anomalies, but the computational requirements and the presence of noise in the coefficient data set must be weighed against the benefits to resolution of the geoid anomaly.

Discussion: Point mass or point dipole

The modeled geoid anomaly in Figure 6b models the disturbing masses as point dipoles using Equation (10) to calculate the spherical harmonic coefficients. The modeled geoid anomaly shows similar patterns of positive and negative geoid anomalies as the observed geoid anomaly in Figure 6a, with negative geoid anomalies corresponding to the northwest-southeast trending San Joaquin Valley to the west of the Sierra Nevada and positive geoid anomalies associated with both the Sierra Nevada Mountains and the coastal mountain ranges of California. While the forward model successfully reproduces the shape of the observed geoid anomaly, the amplitude is suppressed in the modeled geoid anomaly. The lower amplitude of the modeled geoid anomaly in Figure 6b in comparison to the observed geoid anomaly in Figure 6a is possibly due to the

assumption of purely crustal compensation of the Sierra Nevada topography. The distance between the positive and negative poles of the dipole used in the model is limited by the assumption that the balancing mass M_i^- is at the base of the crust. Since seismic studies indicate that the Sierra Nevada Mountains are not underlain by an Airy-style crustal root, the Sierra Nevada could be supported by a compensating mass in the mantle, increasing the distance d between the disturbing mass and the compensating mass and therefore increasing the amplitude of the geoid anomaly. A second set of models was run using the same program to simulate mantle compensation of the Sierra Nevada. By increasing the distance d between the positive and negative poles of the dipole, or the distance between the disturbing mass and the compensating mass, the presence of a compensating mass in the mantle can be simulated. This increase in distance between the poles of the dipole was calculated by increasing the reference crustal thickness in the Airy isostatic calculation. This has the effect on increasing the depth of compensation to simulate the presence of a compensating mass in the mantle instead of placing the compensating mass at the base of the crust. Results from these additional models, using reference thicknesses of 40 and 50 kilometers respectively is shown in Figure 7a and 7b. Figure 7 uses the same color scale as Figure 6 to allow comparison of the amplitudes of the observed geoid anomaly in Figure 6a with the amplitudes of the modeled geoid anomalies for the two models shown in Figure 7. While the increase in the distance between the disturbing mass and the compensating mass results in an increase in amplitude, neither of the models shown in Figure 7 reproduce the amplitude of the observed geoid anomaly from Figure 6a. The increase in amplitude for the models simulating upper mantle compensation of the Sierra Nevada is minimal, indicating that a compensating mass would have to be located much deeper in the mantle to reproduce the amplitude of the observed geoid anomaly.

A second solution to the problem of reproducing the observed geoid anomaly might be found in changing the forward model to calculate the geoid anomaly using a point mass model rather than a point dipole model. Since the Sierras show no evidence of being supported by a thick crustal root and increasing the compensation depth cannot reproduce the amplitude of the observed geoid anomaly without a compensating mass located fairly deep in the mantle, the point dipole model may not be the most appropriate model for the region. Modeling the geoid anomaly using a point dipole model results in the suppression of the amplitude of the geoid anomaly relative to a point mass model. The spherical harmonic coefficients for a point dipole (Equation 10) differ from the coefficients for a point mass (Equation 8) by the scaling factor $-n/(2n + 1)$ and by the ratio d/r_i , the distance between the disturbing mass and the compensating mass divided by the distance of the disturbing mass from the coordinate origin. Since the model assumes crustal compensation of the surface disturbing mass, $d \ll r_i$. The effect of this is that disturbing masses modeled using a point dipole representation have less strength than the same masses modeled using a point mass representation. Reproducing the amplitude of the observed geoid anomalies for the Sierra Nevada by increasing the depth d of the compensating mass requires the compensating mass to be placed fairly deep in the mantle, probably below the base of the lithosphere. This indicates that a point dipole model, and therefore an Airy-style isostatic

compensation model, might not be an appropriate model to apply in the Sierra Nevada Mountains.

Another model: Pratt isostasy

Further application of this model in the area could utilize the crustal thickness data from the seismic studies from the area to test the hypothesis of isostatic support of the Sierra Nevada by a Pratt-style isostatic model. After comparing three simple models to reproduce the observed Bouguer gravity anomaly, Jones et. al. (1994) conclude that the best model for the compensation of the Sierra Nevada is dominated by lateral density variations in the crust, or a crustal Pratt root. In comparison, Wernicke et. al. (1996) conclude that the support of the Sierra Nevada is primarily through lateral density variations in the mantle with small contributions from variations in the crust. Since the current study indicates that Airy-style isostatic compensation fails to reproduce the observed geoid anomaly, the next step would be to modify the forward model to allow for control of the lateral density contrasts in both the crust and the mantle to compare the effects of lateral contrasts in the crust versus the mantle. Pratt-style isostatic compensation might be best modeled by a point mass model, allowing for an increase in amplitude. Additional data on the structure of the crust and mantle could help constrain the model.

Conclusion

The forward model discussed in this paper, while still in its initial stages, has been shown to calculate a reasonable solution to the geoid for isostatically compensated topography. Using spherical harmonics, the model is able to calculate the geoid anomaly for a region at a resolution determined by the limits on the harmonic degree of the solution. The initial assumption made in the model, that topography is isostatically compensated by an Airy-style crustal root, acts as an end member model for the initial tests of the spherical harmonic forward model. Applying the initial end member assumption of Airy isostatic support to the Sierra Nevada indicates that this model fails to completely reproduce the observed geoid anomaly. A different model needs to be applied in the Sierra Nevada since seismic studies in the area indicate the absence of an Airy-style crustal root and the Airy-style compensation models discussed here result in geoid anomalies with suppressed amplitude relative to the observed geoid anomalies. Bouguer gravity anomaly calculations by Jones et. al. (1994) and Wernicke et. al. (1996) indicate that the gravity anomaly can be more accurately modeled using a Pratt isostatic model but there is no agreement on whether compensation is due to lateral variations in the crust or in the mantle or through some combination of the two. The forward model discussed here, since it has proven to produce a reasonable modeled geoid anomaly, can be modified to model the geoid anomaly for other mechanisms of compensation.

References

- Bowin, C.O. (1983), Depth of principal mass anomalies contributing to the Earth's geoidal undulations and gravity anomalies, *Marine Geodesy*, 7(1), 61-100.
- Bowin, C.O., E Scheer, and W. Smith (1986), Depth estimates from ratios of gravity, geoid, and gravity gradient anomalies, *Geophysics*, 51(1), 123-136.
- Chase, C.G. (1985), The geological significance of the geoid, *Annual Review of Earth and Planetary Sciences*, 13, 97-117.
- Featherstone, W.E. (1997), On the use of the geoid in geophysics: A case study over the north-west shelf of Australia, *Exploration Geophysics*, 28(1), 52-57.
- Fliedner, M.M., S.L. Klemperer, and N.I. Christensen (2000), Three-dimensional seismic model of the Sierra Nevada arc, California, and its implications for crustal and upper mantle composition, *Journal of Geophysical Research*, 105, 10,899-10,921.
- Fliedner, M.M. and S. Ruppert (1996), Three-dimensional crustal structure of the southern Sierra Nevada from seismic fan profiles and gravity modeling, *Geology*, 24, 367-370.
- Hager, B.H. (1984), Subducted slabs and the geoid: Constraints on mantle rheology and flow, *Journal of Geophysical Research*, 89, 6,003-6,015.
- Heiskanen, W.A. and H. Moritz (1967), *Physical Geodesy*, W.H. Freeman, San Francisco.
- Jackson, M.J., H.N. Pollack, and S.T. Sutton (1991), On the distribution of anomalous mass within the Earth: Forward models of the gravitational potential spectrum using ensembles of discrete mass elements, *Geophysical Journal International*, 107, 83-94.
- Jones, C.H., H. Kanamori, and S.W. Roecker (1994), Missing roots and mantle "drips": Regional P_n and teleseismic arrival times in the southern Sierra Nevada and vicinity, California, *Journal of Geophysical Research*, 99, 4,567-4,601.
- Pavlis, N.K., S.A. Holmes, S.C. Kenyon, and J.K. Factor (2008), An Earth Gravitational Model to Degree 2160: EGM2008, presented at the 2008 General Assembly of the European Geosciences Union, Vienna, Austria, April 13-18, 2008.
- Pollack, H. N. (1973), Spherical harmonic representation of the gravitational potential of a point mass, a spherical cap, and a spherical rectangle, *Journal of Geophysical Research*, 78(11), 1760-1768.
- Ruppert, S., M.M. Fliedner, and G. Zandt (1998), Thin crust and active upper mantle beneath the Southern Sierra Nevada in the western United States, *Tectonophysics*, 286, 237-252.
- Sutton, S. T., H.N. Pollack, and M.J. Jackson (1991), Spherical harmonic representation of the gravitational potential of discrete spherical mass elements, *Geophysical Journal International*, 107, 77-82.
- U.S. Department of Commerce, National Oceanic and Atmospheric Administration, National Geophysical Data Center (2006), *2-minute Gridded Global Relief Data (ETOPO2v2)*, <http://www.ngdc.noaa.gov/mgg/fliers/06mgg01.html>
- Wernicke, B., et. al. (1996), Origin of high mountains in the continents: The Southern Sierra Nevada, *Science*, 283, 190-193.

Figure Captions:

Figure 1. Basic Airy isostatic compensation model. Variables are defined in Table 1.

Figure 2. Map view of the field point and disturbing mass points. The distance from the field point to all other disturbing mass points is calculated. Disturbing masses within the defined radius of influence contribute to the geoid anomaly at the field point while masses outside of the radius are neglected.

Figure 3. Graphs of relationship between spherical harmonic degree and various parameters. (a) Minimum harmonic degree versus maximum depth of sensitivity as defined by equation 6. (b) Harmonic degree versus wavelength sensitivity as defined by equation 7. (c) Number of coefficients calculated based on maximum harmonic degree. Number of coefficients calculated goes as $(n_{\max} + 1)^2$ (Chase, 1985).

Figure 4. Location and topography of study area. Topography data is from the ETOPO2v2 global topographic grid. Study area is centered on the Sierra Nevada batholith and extends from 35°N to 41°N and 117°W to 122°W.

Figure 5. Predicted crustal thickness in kilometers below sea level in the study area. Topography from ETOPO2v2 generalized to a 10-minute grid shown at bottom left. The predicted crustal thickness was calculated assuming Airy isostatic compensation as defined by equations 2 and 3 and a reference crustal thickness of 30 km. Other variables are defined in Table 1.

Figure 6. Observed and modeled geoid anomaly in meters from harmonic degree $n = 70$ to $n = 905$. (a) Observed geoid anomaly calculated from EGM2008 spherical harmonic coefficient data set (Pavlis et. al., 2008). (b) Modeled geoid anomaly calculated assuming Airy-style crustal compensation of topography with a reference crustal thickness of 30 km and modeling mass anomalies as point dipoles. Both geoid anomaly maps use the same color scale to allow comparison of magnitudes of anomalies.

Figure 7. Modeled geoid anomaly in meters calculated assuming Airy-style isostatic compensation from harmonic degree $n = 70$ to $n = 905$. (a) Modeled geoid anomaly calculated with a reference thickness of 40 km. (b) Modeled geoid anomaly calculated with a reference thickness of 50 km. Both geoid anomaly maps use the same color scale as Figure 6 to allow comparison of magnitudes of anomalies.

Table 1. Variables and values for isostatic compensation

Variable	Description	Value
ρ_c	Crustal density	2750 kg/m ³
ρ_m	Mantle density	3300 kg/m ³
ρ_w	Density of water	1000 kg/m ³
h_r	Reference crustal thickness	30 km
ϵ_c	Elevation	
h_w	Depth below sea level	
h_b	Crustal root thickness	
h_c	Total crustal thickness	

Table 2. Variables used in spherical harmonic and geoid anomaly equations

Variable	Description	Variable	Description
r	distance from coordinate origin to field point	$\bar{P}_{nm}(\mu)$	fully normalized associated Legendre function of degree n and order m
φ	colatitude of field point	$\bar{R}_{nm}(\mu_i, \theta_i), \bar{S}_{nm}(\mu_i, \theta_i)$	fully normalized surface spherical harmonic function of degree n and order m
μ	$\cos(\phi)$	$\bar{J}_{nm}, \bar{K}_{nm}$	coefficients of fully normalized spherical harmonic expansion of gravitational potential
θ	longitude of field point	d	distance between M_i^+ and M_i^- of point dipole
r_i	distance from coordinate origin to i th mass element	G	Newtonian gravitational constant
φ_i	colatitude of i th mass element	M_e	mass of the Earth
μ_i	$\cos(\phi_i)$	r_e	radius of the Earth
θ_i	longitude of i th mass element	$\gamma(\varphi)$	reference gravity as a function of colatitude
M_i	mass of the i th mass element		

Figure 1

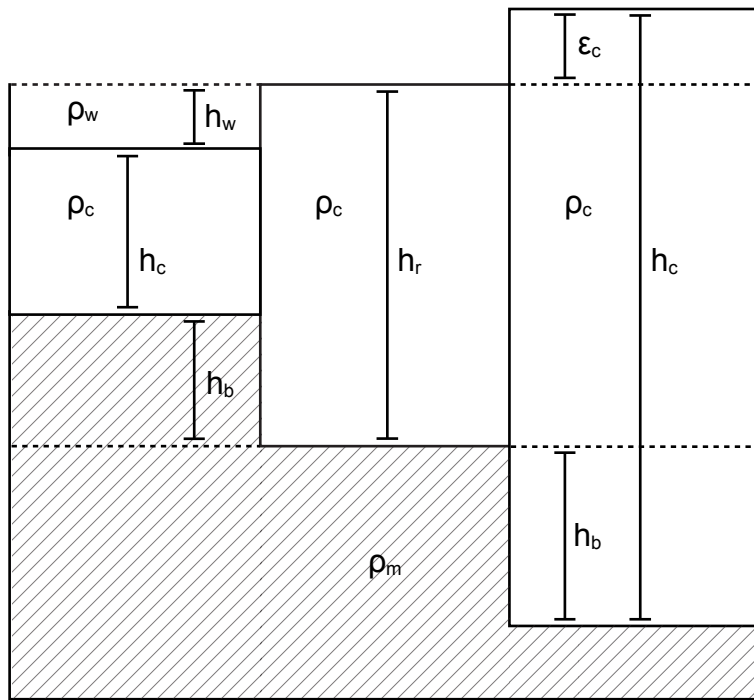


Figure 2

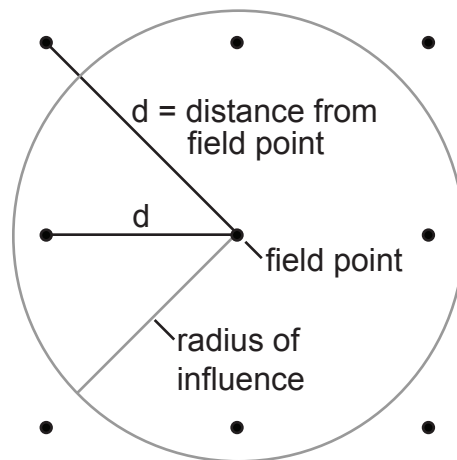
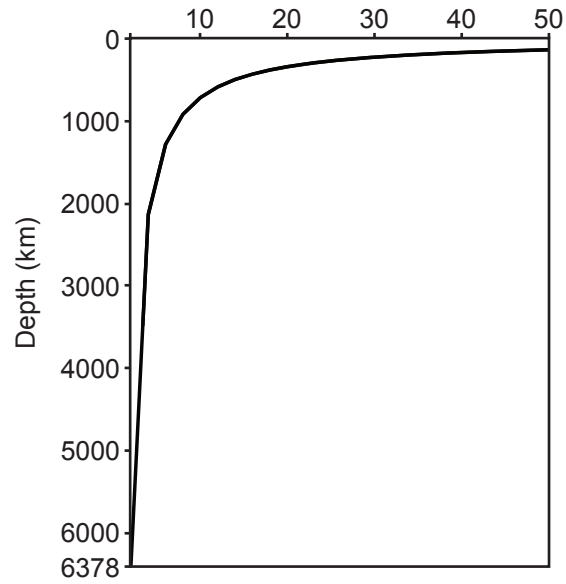
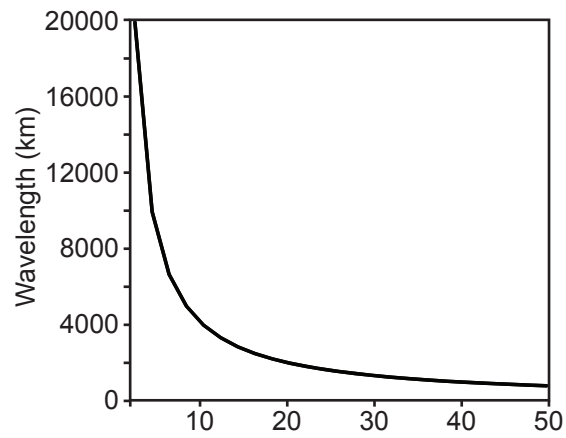


Figure 3

a) Depth sensitivity



b) Wavelength sensitivity



c) Number of coefficients

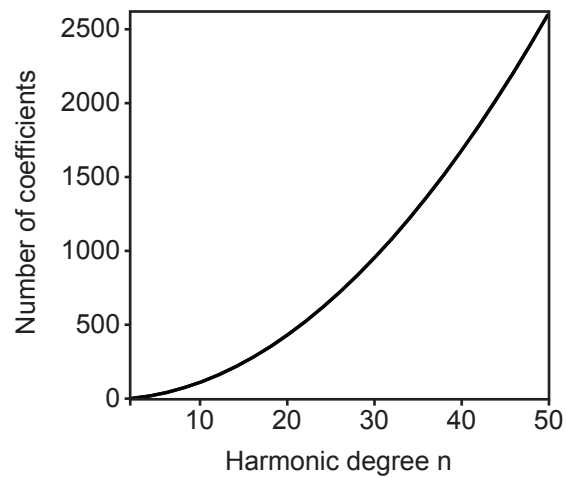


Figure 4

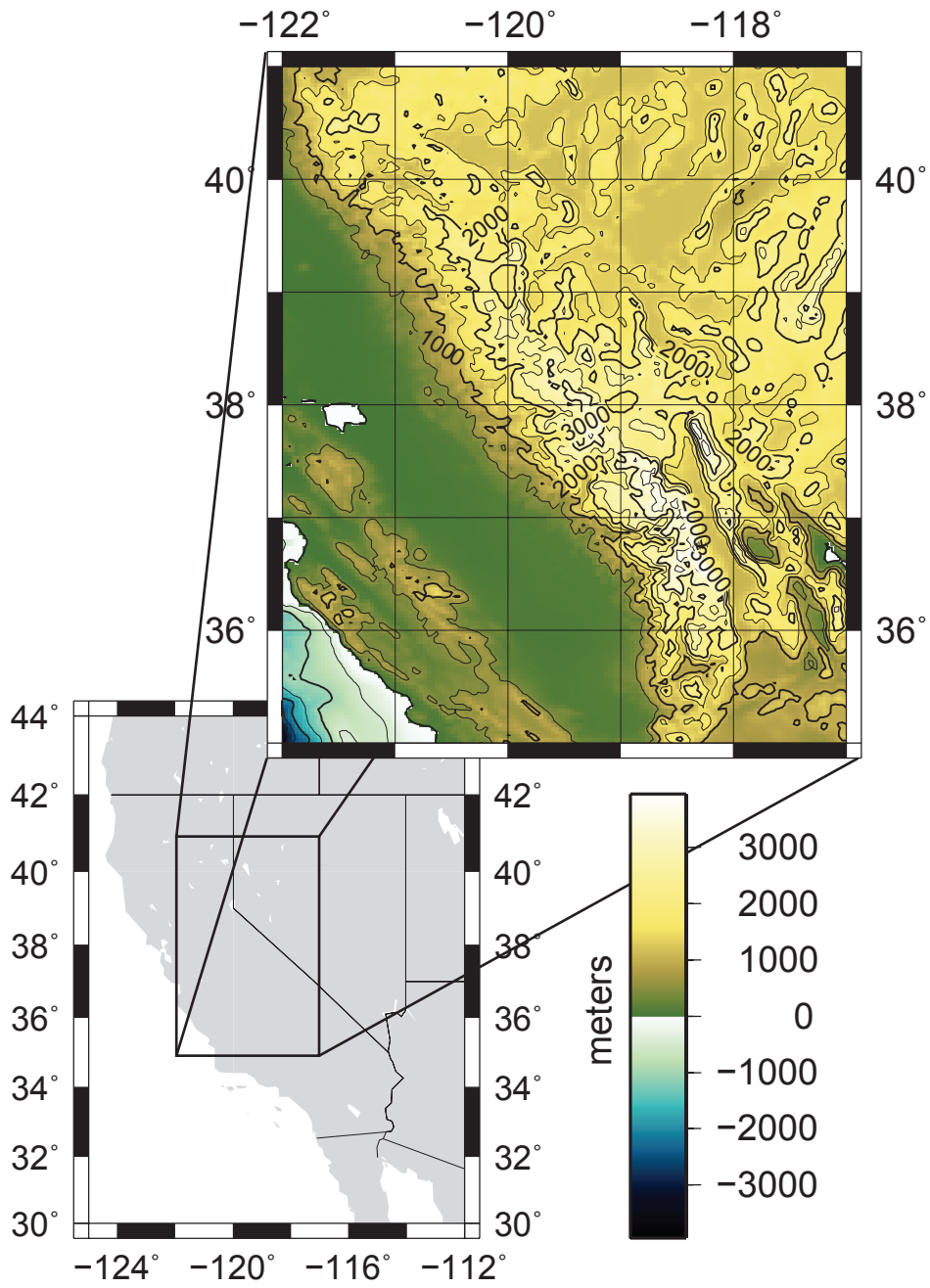


Figure 5

Predicted crustal thickness below sea level with 30 km reference crust assuming Airy-style isostatic compensation

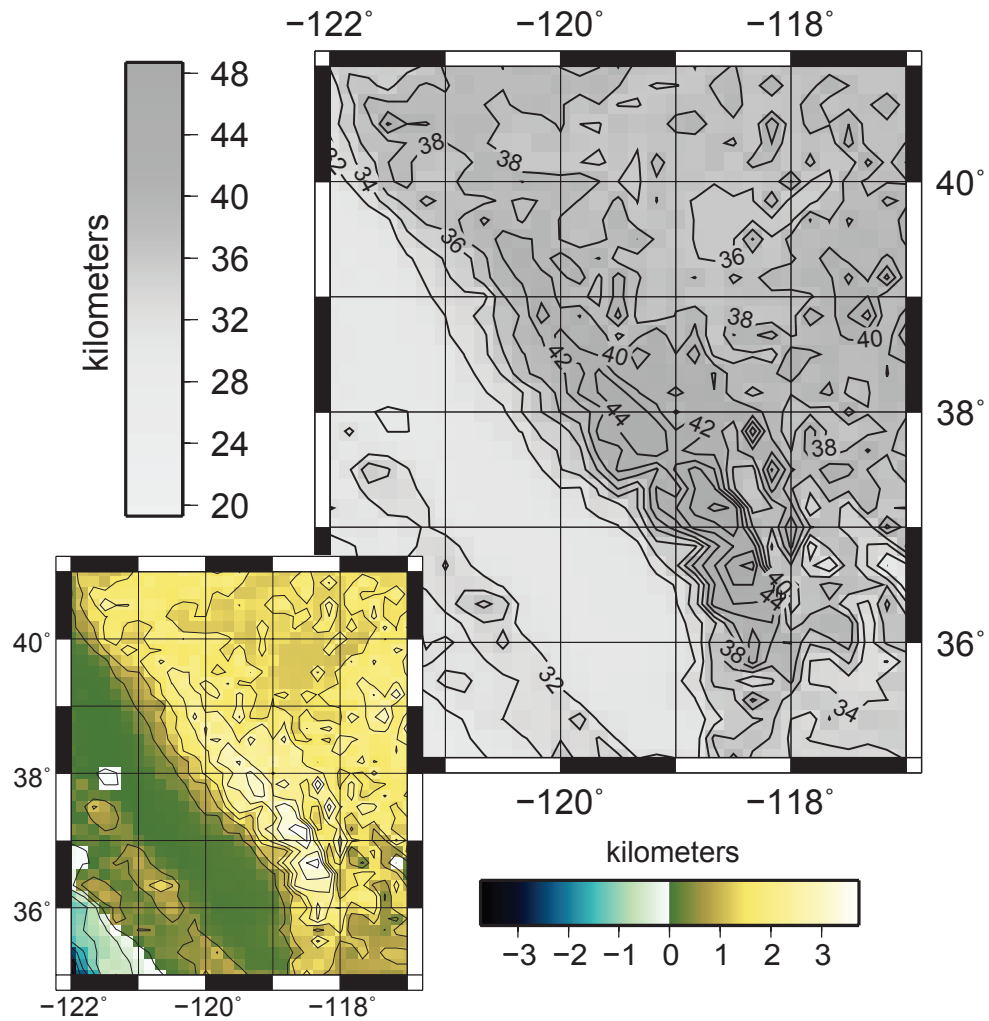


Figure 6

Geoid anomaly from $n = 70$ to $n = 905$

a) Observed geoid anomaly

b) Modeled geoid anomaly
30 km reference crust

